Journal of Applied Volcanology

RESEARCH

Open Access

CNES-ESA satellite contribution to the operational monitoring of volcanic activity: The 2021 Icelandic eruption of Mt. Fagradalsfjall

Mathieu Gouhier[1*], Virginie Pinel[2], Joaquín M. C. Belart[3,4], Marcello De Michele[5], Catherine Proy[6], Claire Tinel[6], Etienne Berthier[7], Yannick Guéhenneux[1], Magnus Tumi Gudmundsson[4], Birgir V. Óskarsson[8], Shan Gremion[9], Daniel Raucoules[5], Sébastien Valade[10], Francesco Massimetti[11] and Bjorn Oddsson[12]

Abstract

Within the framework of the CIEST[2] (Cellule d'Intervention d'Expertise Scientifique et Technique new generation) and thanks to the support of CNES, the French space agency, the first phase of the Fagradalsfjall eruption was exceptionally well covered by high resolution optical satellite data, through daily acquisitions of Pléiades images in stereo mode. In this study, we show how Pléiades data provided real-time information useful for the operational monitoring of the ongoing eruption. An estimation of the volume of lava emitted as well as the corresponding effusion rate could be derived and delivered to the civil protection less than 6 h after the data acquisition. This information is complementary to and consistent with estimates obtained through the HOTVOLC service using SEVIRI (Spinning Enhanced Visible and Infrared Imager) sensor on-board Meteosat Second Generation (MGS) geostationary satellites, operated by the European Space Agency (ESA), characterized by a lower spatial resolution and a higher temporal one. In addition to the information provided on the lava emission, Pléiades data also helped characterize the intensity of the eruption by providing insight into the elevation and the velocity of the volcanic plume. The survey of this effusive eruption, well anticipated by a series of precursors, is a proof of concept of the efficiency of optical/thermal satellite data for volcanic crisis real-time monitoring.

Keywords: Volcanology, Remote sensing, Pléiades images, Infrared monitoring, Lava

Introduction

Lava flows on the ground and related atmospheric ash/SO_2 emissions induced by the volcanic activity are common hazards occurring during eruptions and can represent a threat to the population living in the vicinity of volcanoes areas (e.g., Allen et al., 2000; Vicari et al., 2011). Effusion rates and degassing are key information on the intensity of the eruption, the driving forces leading to magma ascent and thus the temporal evolution of the event. Today, operational monitoring of volcanic products is achieved through both in-situ measurements and ground-based instruments (Marzano et al., 2006; Calvari et al., 2011; Gouhier et al., 2012; Aiuppa et al., 2015; Di Traglia et al., 2021). The development of ground-based remote sensing tools, such as those aimed at studying lava flows propagation, open vent degassing, or ash emissions are now part of routine monitoring operations at many volcanoes (Scollo et al., 2009; Barsotti et al., 2020; Peltier et al., 2021; Kelfoun et al., 2021). However, for volcanoes

*Correspondence: M.Gouhier@opgc.fr

[1] Université Clermont Auvergne, CNRS, F-63000 Clermont-Ferrand, IRD, OPGC, LMV, France
Full list of author information is available at the end of the article

located in remote areas, where the installation and maintenance of expensive instruments network is difficult, satellite-based techniques are more beneficial if satellite remote sensing systems can provide a rapid assessment of volcanic activity (Schmidt et al., 2015; Gouhier et al., 2016; Coppola et al., 2016a, b; Dumont et al., 2018; Valade et al., 2019; Albino et al., 2020). This is particularly important as such data can potentially be used to derive crucial information for decision makers. Yet the provision of accurate data in a timely fashion remains very challenging from space as sensors on-board Low-Earth Orbiting (LEO) platforms with very high spatial resolutions usually have low frequency of acquisition (such as Pléiades), while sensors on-board geostationary (GEO) platforms with very high acquisition rate suffer from low spatial resolution (such as MSG satellites).

Satellites have already been extensively used to produce digital elevation models (DEMs) in volcanic areas and infer the volume of eruptive deposits by comparing the differences between a DEM obtained after the emplacement of deposits with a pre-eruptive DEM. While most studies are based on TanDEM-X bistatic radar data (e.g. Albino 2015, Bato 2016, Albino 2020), some use high-resolution Pléiades optical data acquired in stereo mode (Bagnardi et al 2016; Carrara et al 2019). For the October 2010 effusive eruption of Piton de la Fournaise, Réunion Island, Bato et al, (2016) made a direct comparison of mean effusion rates derived by DEMs differentiation and by thermal anomalies quantification from MODIS data and demonstrated a fairly good agreement between the two independent dataset. While the growth rate of domes has been estimated from Pléiades imagery (Pinel et al., 2020; Moussallam et al, 2021), until now, optical satellite imagery has never been used to estimate the temporal evolution of the volume of magma emitted during a lava flow emplacement event, providing only an estimate of the total volume of the emplaced lava flow. However, there are a few examples of studies providing the temporal evolution of the eruptive rate based on TanDEM-X data (e.g. Poland 2014, Arnold 2017, Kubanek 2017). However, all these studies were performed a posteriori and, so far, satellite imagery has never provided real-time DEMs for operational monitoring. The time evolution of effusion rates can also be obtained from MidWave InfraRed (MWIR) satellite imagery either from LEO platforms such as Terra-MODIS providing time-average effusion rates (Wright et al., 2001; Coppola et al., 2016a, b), or from GEO platforms such as Meteosat-SEVIRI, providing instantaneous effusion rates (Ganci et al., 2012; Gouhier et al., 2016). A comparison of the cumulative volume estimated by SEVIRI and DEM difference has been performed a posteriori for the 2015 eruption of Etna (Ganci et al. 2019a). The volume derived from SEVIRI data was 20% smaller than that estimated from the difference between DEMs, which was interpreted by the authors as resulting from lava porosity. Interestingly, Sentinel-2 satellite (ESA-Copernicus) providing ShortWave InfraRed (SWIR) data fills the gap between Pléiades Optical and Meteosat MWIR data in terms of temporal and spatial resolutions. In particular, it allows an attractive compromise for the monitoring of effusive eruptions and the cartography of lava flow field (Valade et al., 2019; Massimetti et al., 2020). Finally, the coherence of radar data can also be used in real time to derive the evolution of the surface covered by the lava (Ebmeier et al., 2012; Kubanek et al., 2015; Valade et al., 2019; Richter and Froger 2020).

In order to promote the use of satellite data for hazards studies and mitigation, two French initiatives have been undertaken. (i) The Technical-Scientific Intervention and expertise unit (CIEST^2 – Cellule d'Intervention d'Expertise Scientifique et Technique) new generation, was created in 2019 following the expression of interest of about 30 French scientists. The objective is to extend and facilitate the acquisition and use of very high optical images from Pléiades acquired under the International Charter "Space and Major Disasters", for the understanding and study of geological hazards. The CIEST^2 initiative is now placed in the framework of the solid Earth national data and services pole Form@ter. (ii) In parallel, HOTVOLC is a geostationary satellite-data-driven service dedicated to the real-time monitoring of active volcanoes, allowing lava hot spots, ash and SO_2 clouds products to be detected and tracked at an acquisition rate of one image every 15 min (Gouhier et al., 2016; 2020). HOTVOLC uses Meteosat-SEVIRI infrared images and is part of the National Observation Service for Volcanology (SNOV – Service National des Observations en Volcanologie) operated by the CNRS (Centre National de la Recherche Scientifique). Its mission is to ensure continuous and permanent monitoring of French volcanoes, as well as volcanic targets (Italy, Iceland, Lesser Antilles, etc.) whose products may affect French territories.

In this context, the recent Icelandic eruption of Mt. Fagradalsfjall in the Reykjanes Peninsula, which started on March 19, 2021 offers a very good opportunity to demonstrate the ability of the CIEST^2 and HOTVOLC initiatives to provide a rapid and concerted response to gather crucial information useful for making informed decisions. The Fagradalsfjall eruption was closely monitored with remote sensing data through the CIEST^2, HOTVOLC and MOUNTS initiatives during the first 10 days of the eruption, and through the entire eruption using a large amount of airborne data (Pedersen et al., 2022). The eruption is a long-term basaltic effusive eruption that initiated as a fissure eruption on 19 March 2021 within an enclosed valley, accompanied by small lava fountains which ended on 18 september. In this paper, we present the two French initiatives CIEST^2 and HOTVOLC with associated methodology, and discuss their capabilities and limitations, as well as the major interest of coupling these two approaches. We also present the potential contribution of Sentinel-2 data for the estimation of lava surface from the operational platforms MOUNTS. Then, we describe the results obtained from Pléiades and Meteosat data. This comprises, in particular, the estimation of lava flows volume and volcanic plume elevation from Pléiades DEMs, as well as the comparison between average and instantaneous lava discharge rates using Pléiades and Meteosat images, respectively. We also provide airborne data at very high spatial resolution, hereafter used as a validation of satellite-based products.

Operational initiatives for a rapid response using CNES/ESA spatial resources

CIEST^2: Technical-Scientific Intervention and expertise unit

CIEST^2 is a French initiative aiming at fostering cooperation of the geophysical community around the use of satellite imagery for geohazards monitoring and understanding. This synergy between CNES (the French Space Agency) and the French "solid Earth" community aims at a quick response in the programming and use of Earth observation resources, in the event of a geophysical hazard. The goal of the initiative is to analyze and process space imagery to ultimately improve our knowledge of a geophysical phenomenon.

CIEST^2 initiative started in 2005 as a formal agreement between six national organizations (BRGM, CEA, INSU, IPGP, IRD, UCBL) which aimed to extend the use of space resources, in particular the SPOT images acquired within the framework of the International Charter on Space and Major Disasters, for the study and understanding of geophysical hazards. Today (2022) the CIEST^2 initiative has become a synergistic working group based on very high resolution Pléiades stereo images provided by CNES and potentially Copernicus Sentinel-1 and -2 data. The organization is as follows: In case of events such as earthquake, volcano eruption, landslides or glacier collapse, the CIEST^2 steering committee decides to activate the CIEST^2 device. Then, CNES immediately triggers Pléiades stereo tasking by Airbus Defense and Space (Airbus DS) in order to enable DEM generation or multi-temporal analysis. The acquisition strategy chosen consists of pointing the Pléiades-1A and -1B satellites systematically at each passage over the area. For 10 consecutive days, daily acquisitions in "stereo" mode take place, exploiting the agility of the satellite, capable of pointing its optical system towards any target located in its field of view. Each acquisition consists of a pair of two images, taken with different viewing angles, less than a minute apart from the same orbit, in order to increase the chances of obtaining a visual, and, if applicable, to be able to calculate the topography of the area of interest by stereo-photogrammetry.

HOTVOLC: Geostationary-data-driven operational service

HOTVOLC is a Web-GIS (Geographic Information System) volcano monitoring system (Fig. 1) using SEVIRI (Spinning Enhanced Visible and Infrared Imager) sensor on-board METEOSAT geostationary satellite (https://hotvolc.opgc.fr) and developed at the OPGC (Observatoire de Physique du Globe de Clermont-Ferrand) in 2009 after the installation of the first receiving station. The spectral bands of the SEVIRI sensor allow the HOTVOLC system to simultaneously characterize volcanic ash, sulfur dioxide, and lava flow emissions. It is designed for the real-time monitoring of ~ 50 active volcanoes and provides high value-added products at the frequency of one image every 15 min with a pixel resolution of 3 × 3 km at nadir. HOTVOLC is open-access and data can be downloaded from the entire database covering the period 2010–2021. Satellite products are delivered in the form of (i) geo-referenced images (geotiff) tiled on a background map, and (ii) time series (csv) associated with interactive data visualization technologies. HOTVOLC is part of the SNOV and is labelled by the CNRS since 2012. Within this framework we ensure real-time monitoring of French volcanic targets, as for Piton de la Fournaise effusive eruptions (e.g., Peltier et al., 2021; Thivet et al., 2020). Also, we provide timely information on other volcanic targets whose products may affect French territories such as the Icelandic 2010 Eyjafjallajökull eruption (e.g., Bonadonna et al., 2011; Labazuy et al., 2012), whose volcanic ash plumes reached the French airspace. Since 2018, HOTVOLC falls under the official function of Meteo-France (Gouhier et al., 2020) and provides data to the Toulouse VAAC (Volcanic Ash Advisory Centre) allowing a better assessment of the risk related to air traffic. Figure 1 is a screenshot of the HOTVOLC Web-GIS interface, showing the first hot spot anomaly detected by the system on March 19, at 21h15 UTC, i.e., only 30 min after the 2021 Fagradalsfjall eruption start, and which evidences the arrival of lava flows on the surface.

MOUNTS: Sentinel-Copernicus operational service

MOUNTS (Monitoring Unrest from Space, Valade et al. 2019, www.mounts-project.com) is an operational volcano monitoring system using the polar-orbiting ESA Copernicus Sentinel satellite constellation (Sentinel-1, -2, -5P), together with Deep Learning, to assist in specific processing tasks. The synergistic use of radar (Sentinel-1 Synthetic Aperture Radar SAR), short-wave infrared (Sentinel-2 MultiSpectral Instrument MSI) and

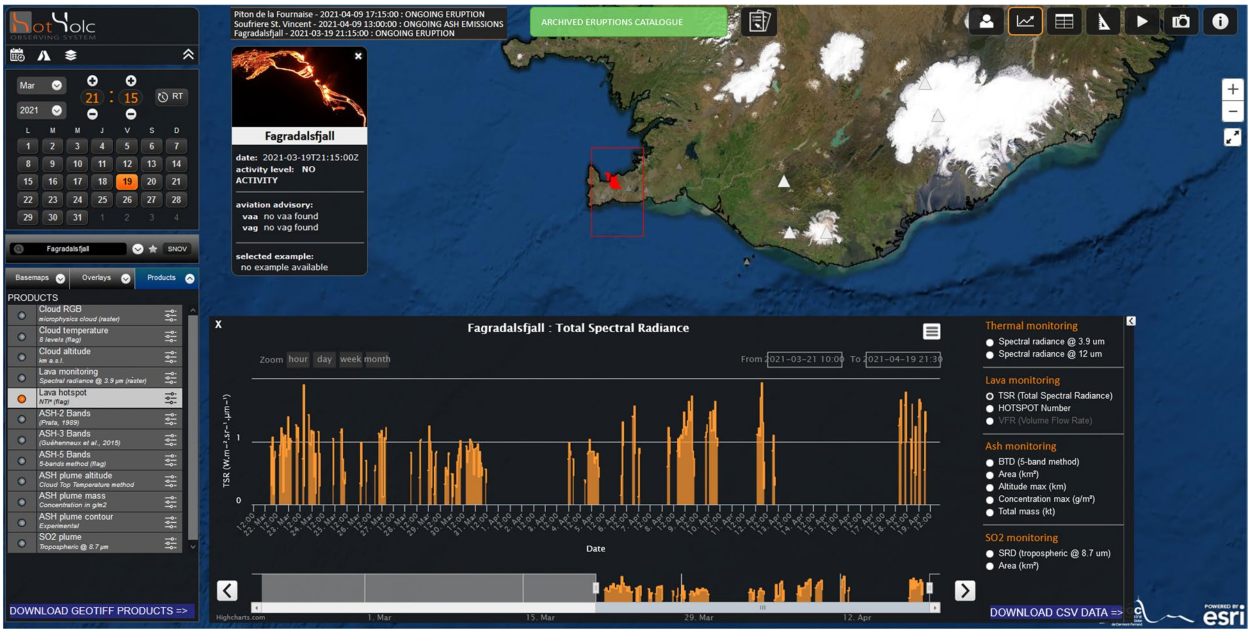

Fig. 1 Screenshot of the HOTVOLC Web-GIS interface (https://hotvolc.opgc.fr) showing the hot spot anomalies (red pixels) in the Reykjanes peninsula 45 min after the onset of the eruption on March 19, 21h15 UTC. Below, one can observe a time series of the total spectral radiance spanning one month of effusive activity

ultraviolet (Sentinel-5P TROPOMI) payloads, allows for monitoring on a single web-interface of surface deformation, topographic changes, emplacement of volcanic deposits, detection of thermal anomalies, and emission of volcanic SO_2. The web-design is inspired by the MIROVA volcano monitoring system (Coppola et al. 2016a, b), whereby monitored products are delivered in the form of images and time series, with interactive tools added to ease the data visualization (Fig. 2). The system currently monitors over 70 volcanoes worldwide, but the number is regularly increasing as its flexible design allows for rapid addition of new volcanoes in response to volcanic unrest in any part of the globe.

In this study we will only present Sentinel-2 data from MOUNTS, here used to derive information on lava flow field emplacement. Sentinel products are automatically downloaded from the Copernicus Open Access Hub as soon as they are available (typically 2–12 h from sensing for Sentinel-2 L1C products), and immediately processed and published on the MOUNTS website (typically 0.5–3 h after availability online). Sentinel-2 images are acquired from two polar-orbiting satellites (Sentinel-2A and -2B, launched in 2015 and 2017 respectively), and placed 180° from each other in the same sun-synchronous orbit. The revisit time is 5-days on average (reduced to 2–3 days at mid-latitudes), with spatial resolution of 20 m/pixel in the SWIR bands and 10 m/pixel in the optical bands.

Methodology

Pléiades data

The data collected by Pléiades during 22–31 March 2021 (days 3 to 13 after the start of the eruption) were tasked by Airbus DS and CNES in "emergency mode". During this time period, the satellite imaged the area of interest daily between 12:50–13:30 local time, and the images were available for download about 2 h after the acquisition. Table 1 lists the characteristics of the subset of images for which the eruption site was cloud free.

Mapping the lava area, volume and effusion rate

Once downloaded, we processed a subset of the images using the Ames StereoPipeline (ASP, Shean et al., 2016) with the correlation parameters defined by Deschamps-Berger et al., (2020). The processing pipeline included the use of a reference DEM, which constrains the matching algorithms in the photogrammetric processing. For reference, we used the IslandsDEMv0 from the National Land Survey of Iceland (atlas.lmi.is/dem). The IslandsDEM is a seamless 2 × 2 m DEM mosaic with improved spatial accuracy compared to the ArcticDEM (Porter et al., 2018), by merging repeated ArcticDEM acquisitions in order to minimize outliers.

The processing time with ASP of each Pléiades stereopair was < 30 min (AMD Ryzen Threadripper 3970X 32-Core Processor, 128 Gb Memory). The resulting DEM, with 2 × 2 m Ground Sampling Distance (GSD)

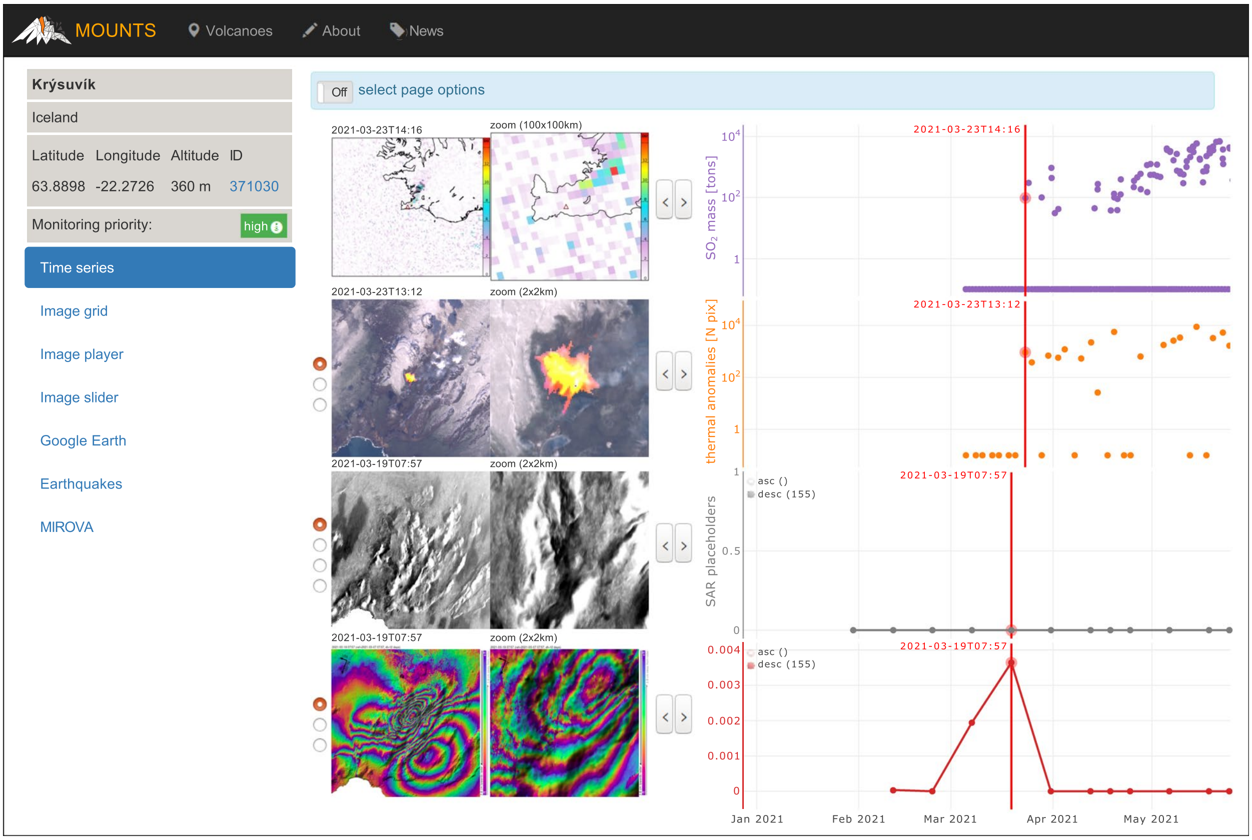

Fig. 2 Screenshot of the MOUNTS interface (www.mounts-project.com) showing Sentinel data images and time series in the Reykjanes peninsula at the onset of the eruption

Table 1 Characteristics of Pléiades acquisitions (all in stereo mode) with good visibility (limited cloud cover) over the eruption site and used to estimate the volume of the lava field between days 3 and 13 after the eruption started

Acquisition time	Along track incidence angles	Across track incidence angles	B/H
22 March 2021 13:23	-5.4 5.2	13.4 13.6	0.19
23 March 2021 13:15	-6.7 8.5	6.1 7	0.29
26 March 2021 12:52	-3.2 3.5	-14.4 -13.9	0.13
29 March 2021 13:19	-3.2 3.6	9.9 10.5	0.13
30 March 2021 13:11	-5.5 5.3	2.8 3.5	0.21

was co-registered to the IslandsDEMv0 using the co-registration method by Nuth & Kaab (2011), implemented in python by D. Shean (https://github.com/dshean/demcoreg, Shean et al., 2016), and the corresponding orthoimage, with 0.5 × 0.5 m GSD, was shifted horizontally by the same vector. Lava outlines were manually digitized from the co-registered Pléiades orthoimage. The difference in elevation between each Pléiades DEM and the IslandsDEM resulted in a lava thickness map, which was subsequently cropped using the lava outlines. This allowed the calculation of the lava volumes, by estimating an average thickness value multiplied by the area of the lavas. The uncertainties in the lava volume were estimated using the Normalized Mean Absolute Deviation (NMAD, Höhle and Höhle, 2009) in the unchanged areas around the eruption site, conservatively assuming this value as the uncertainty in the average lava thickness. The lava area, volume and effusion rate were reported to the Icelandic Civil Protection typically by or before 18:00 local time, i.e., less than six hours after the Pléiades acquisitions.

In addition to this rapid processing performed in "response mode", DEMs were calculated, a posteriori, either using ASP with various processing strategies or with the online service DSM-OPT [developed by D. Michéa et J.-P. Malet / EOST; E. Pointal, IPGP] based on MicMac (Rupnik et al., 2017). The preferred processing scheme in reanalysis mode was based on the ASP processing scheme described in Shean et al., (2021a) and Shean et al., (2020) using the More Global

Matching correlation algorithm. This provided the best tradeoff between data gaps, data outliers, smoothness and sharpness of the terrain. The DEMs produced in reanalysis mode were also corrected for along-track jittering errors (e.g. Girod et al., 2017; Deschamps-Berger et al., 2020) using a methodology inspired from Berthier et al. (2007) similar to the one described in Shean et al., (2021b).

Mapping the elevation of the volcanic cloud

The algorithm employed was mainly developed and presented by the authors in de Michele et al. (2016; 2019). Here, it is applied to Pléiades images acquired on the Fagradalsfjall eruption on the, 23 of March 2021. The methodology takes advantage of the spatial offsets of the linear sensor arrays of different bands on-board the satellite's push-broom image scanner, which results in multiple images with very short time difference acquired at the same date. In particular, there are 0.16 s delay between the panchromatic band (PAN) recording reflected light at 480–820 nm and the multispectral band 2 (B2) recording light at 620–700 nm (the human interpret this range of wavelengths as the color « red»). Since the satellite platform is flying at a ~ 7 km/s, there is a baseline of 1.12 km between PAN and B2 recording. Pléiades is orbiting at a nominal altitude of 694 km, therefore there is a base to height ratio (B/H) equal to 0.001613. This B/H is enough to enable stereoscopic view and restitute the altitude for objects higher than 120 m, given that the precision of the correlator is $1/10^{th}$ of a pixel (i.e. 20 cm for B2). The PAN image pixel size is 0.5 m while the B2 pixel size is 2 m. The first step of our process consists in resampling the PAN image on B2 image. Then, we calculate pixel offsets with subpixel precision, in the epipolar direction (O_e) and in the perpendicular-to-epipolar direction (O_{p2e}). Afterwards, we measure the volcanic cloud direction (Θ) with respect to the O_{p2e} direction. Finally, we calculate the digital elevation model of the volcanic cloud, the Plume Elevation Model (PEM), and its horizontal velocity by applying the following formula to the offsets map:

$$h = \left(|O_e| - \left|O_{p2e}\right||tan\theta|\right).\frac{s.H}{V.t}$$

h is the height (m), *s* is the pixel size (m), *V* is the platform velocity (m/s), *t* is the temporal lag between the Pléiades bands (s) and *H* is the platform height (m). The minus occurs because theta is – in the present case—between zero and 180°, as explained in de Michele et al., (2019). The horizontal velocity along the plume axis is:

$$v = O_{p2e}S/t.cos\theta$$

with two peculiar cases described as follows:

- θ ~ 0° and θ ~ 180°. Under these conditions, the system is no longer sensitive to plume velocity, thus:

$$h = (|O_e|).\frac{s.H}{V.t}$$

- θ ~ ±90°. No relation between plume velocity and $|O_e|$. Therefore, the effect of the plume velocity cannot be compensated.

This method works only if the volcanic cloud is visible (opaque volcanic clouds only).

Airborne data.

As part of the response plan, made in early March, airborne photogrammetric surveys have been taking place over the entire Mt. Fagradallsfjall area. A medium-format Hasselblad A6D 100MP camera with a HC 3,5/35 mm lens was used on-board a TF-KLO Cessna C172N in two flights before the eruption and on the flights of the 20^{th} and 23^{rd} of March, and the remaining flights on-board a twin propeller/high-wing TF-BMW Vulcanair P68 Observer 2 survey aircraft operated by Garðaflug (Pedersen et al., 2022). The flights collected vertical aerial photographs at a 3–6 s interval 2000–6000 feet above ground, ensuring an overlap of 70% to 90% between photographs along a flightline. These photographs were processed using MicMac (Pierrot Deseilligny et al., 2011, Rupnik et al., 2017), in a semi-automated workflow following the steps described by Belart et al., (2019). The photogrammetric processing required the digitization of Ground Control Points (GCPs). The GCPs were extracted from an orthomosaic and a DEM obtained from a previous photogrammetric survey done on the 7th of March, with similar level of detail as the photogrammetric surveys carried out during the eruption. The data was processed into a DEM of 1x1 m GSD and an orthomosaic of 0.2x0.2 m GSD, which allowed retrieval of areal coverage, lava volume, lava thickness and effusion rate in a similar manner as described in Sect. 3.2 for the Pléiades stereoimages.

The setup of the airborne surveys improved in early-April, when a series of targets were emplaced in the field and measured by GPS (RTK mode), intended to be used as GCPs and producing higher positional accuracy in the resulting DEMs and orthomosaics. The DEM and orthomosaic from 18 May 2021 were used as reference to extract GCPs and, used to reanalyze the airborne surveys of the first weeks of the eruption.

MSG-SEVIRI lava volume flow rate

In this study, we take advantage of the HOTVOLC system in order to early-detect and track lava hot spots related to the emergence of the lava flow at the surface and then, provide instantaneous lava Volume Flow Rates, hereafter referred to as VFR. Fagradalsfjall is located on the northern edge of the Meteosat Field Of View (FOV), hence having a weak spatial resolution with a nominal pixel area of about 48 km^2. Early detection of lava hot spots at this resolution is very challenging and already shows that Low-Earth Orbiting (LEO) platforms can be of great help in these particular cases. In order to address the issues related to low spatial resolution, bad weather or changing conditions of acquisition, we developed a detection procedure based on a contextual algorithm that uses a modified Normalized Thermal Index (NTI*). It adapts the original NTI as developed by Flynn et al. (2002) and combines the Mid Wave InfraRed (MWIR) band at 3.9 μm and the Thermal InfraRed (TIR) band at 12 μm. Moreover, the fixed threshold proposed by Wright et al. (2002) was abandoned in favour of a dynamic threshold which adapts to the spatial and temporal variability of NTI* (Gouhier et al., 2016). The combination of all these properties (spectral spatial and temporal) allows us to detect hot spot anomalies even for newly emplaced lava flows which represents a very small fraction of the pixel.

Lava discharge rates have been estimated using instantaneous lava volumes, calculated from infrared techniques. This method is based on the mass conservation principle and benefits from a rapid succession of images obtained using geostationary satellites. The physical principle is as follows: the pixel-integrated thermal anomaly measured at a given instant is the balance of contributions related to (i) hot lava material newly emplaced (at time *t*) and (ii) cooling lava material previously emplaced (at time *t-1*). This problem can be addressed using the mass conservation principle following the differential equation:

$$\frac{dV(t)}{dt} = Q(t) - kV(t)$$

V is the total volume of lava in a given image, *Q* is the lava volume flow rate (i.e., source term) and –*kV* is the loss term with *k* representing the lava cooling rate (s^{-1}). Note that satellite observations provide discrete time series, to obtain *Q* we thus solve analytically the above differential equation with Δt being the time interval between two consecutive images such that:

$$Q(t) = k\frac{V_i - V_{i-1}e^{-k\Delta t}}{1 - e^{-k\Delta t}}$$

The cooling rate *k* is often expressed as $k = 1/\tau$, where τ is the lava e-cooling time. This method, referred to as the Volume Flow Rate (VFR) method, allows the calculation of quasi-instantaneous lava effusion rates (in m^3/s). The quantification of instantaneous lava effusion rates is essential as it strongly controls the lava front speed and flow area. Moreover, the short-term evolution of lava effusion rate traduces eruptive dynamics changes from shallow depth to the surface.

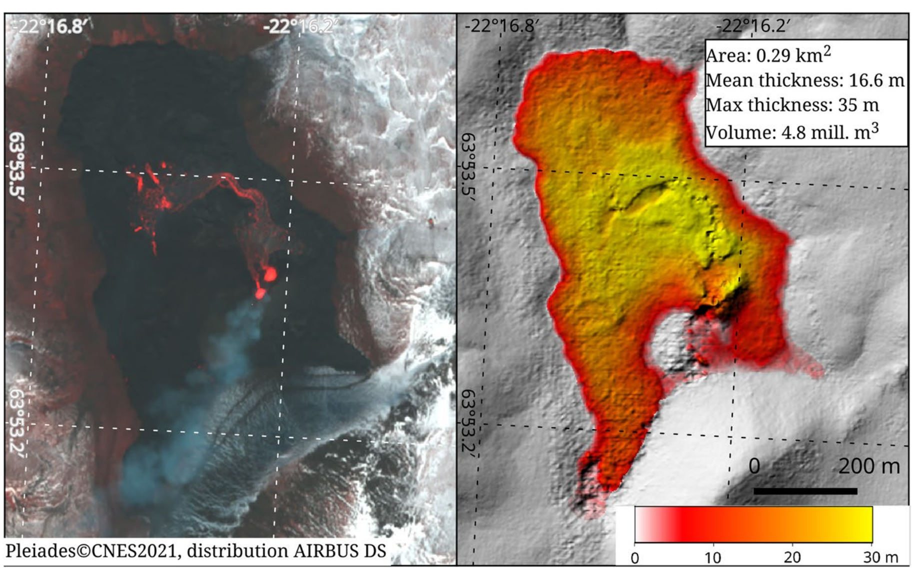

Fig. 3 Left panel: Pléiades multispectral image acquired on the 30th of March 2021, Right Panel: lava thickness derived by differentiating the DEM produced in response mode from the images acquired on the 30th of March 2021 and the pre-eruptive arctic DEM. Background: hillshade of the 30th March DEM. © CNES 2021, Distribution Airbus DS

Table 2 Total lava volumes calculated from Pléiades and airborne stereoimages, in response-mode and reanalysis-mode, using the Islands DEM as the pre-eruption DEM. Volumes are expressed in million cubic meters. All the effusion rates are reported as an average since the start of the eruption, defined on 19 Mar 2021, 21:40 local time

Survey	Response mode		Reanalysis mode	
	Volume (Mm^3)	Avg eff. Rate ($m^3\ s^{-1}$)	Volume (Mm^3)	Avg eff. Rate ($m^3\ s^{-1}$)
20210322_1323 (Pléiades)	1.43 ± 0.09	6.2 ± 0.4	1.39 ± 0.09	6.0 ± 0.4
20210323_1010 (Airborne)	1.72 ± 0.09	5.6 ± 0.3	1.90 ± 0.06	6.2 ± 0.2
20210323_1315 (Pléiades)	1.84 ± 0.08	5.8 ± 0.3	1.94 ± 0.07	6.2 ± 0.2
20210326_1252 (Pléiades)	3.30 ± 0.21	5.7 ± 0.4	3.22 ± 0.16	5.6 ± 0.3
20210329_1319 (Pléiades)	4.57 ± 0.11	5.4 ± 0.1	4.54 ± 0.14	5.4 ± 0.2
20210330_1311 (Pléiades)	4.89 ± 0.10	5.3 ± 0.1	4.90 ± 0.11	5.3 ± 0.1
20210331_1206 (Airborne)	5.23 ± 0.14	5.2 ± 0.1	5.19 ± 0.11	5.2 ± 0.1

Sentinel-2 hot spots detection

The Sentinel-2 MSI satellite images, are analyzed by applying a recent volcano-dedicated, automated and global hot spot detection algorithm based on fixed ratios in the shortwave infrared (SWIR), with a contextual threshold derived from a statistical distribution of anomalous pixel clusters (Massimetti et al., 2020). The aim of the algorithm is to precisely detect the hottest portion, directly related to the ascent of magmatic fluids subaerially exposed, and to quantify the number of thermally active pixels, or in other words the radiant emitting hot area of a lava body. Indeed, SWIR signals (1.1 to 3.0 μm) record almost purely thermal emissions produced by hot emitting surfaces (Harris, 2013; Blackett, 2017). Sentinel-2 dataset (Level 1C Product) is analyzed considering the SWIR top-of-atmosphere (TOA) reflectances in the ρ12 (2.19 μm), ρ11 (1.61 μm), and ρ8A (0.86 μm) bands. The algorithm runs to detect the number of "hot" pixels, where a hotter area is superficially exposed (T > 200 °C ca.), with an overall estimate of 2 – 4% false alerts detected (Massimetti et al., 2020). The reliability of the applied algorithm has already been successfully tested, firstly with a direct comparison to volcanogenic heat flux (in Watt) through MODIS Middle Infrared images; and

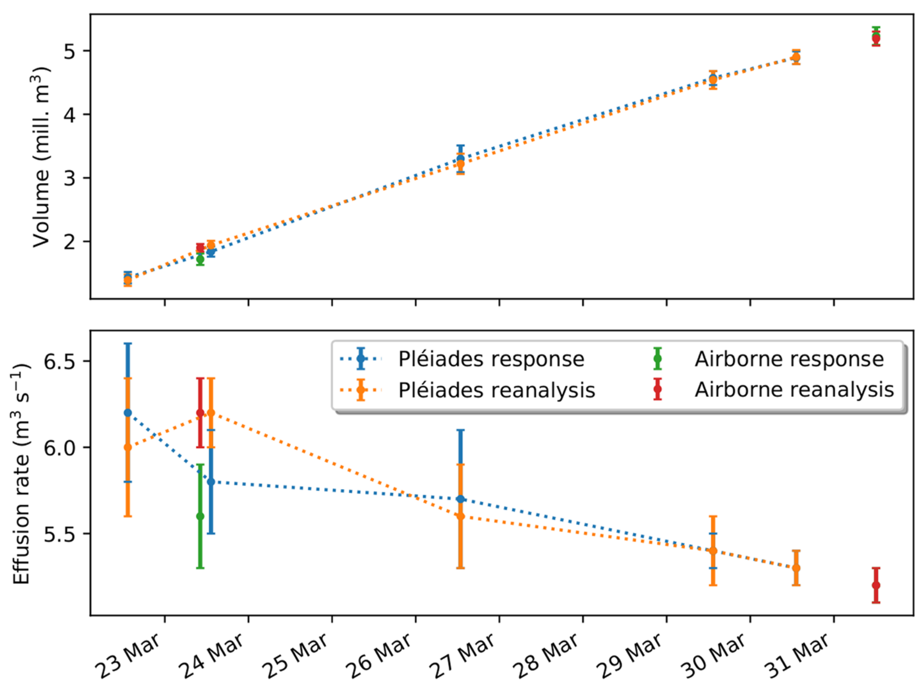

Fig. 4 Lava volume and effusion rate (average since the start of the eruption) calculated in response mode and in reanalysis mode

then on a variety of different volcanological thermal-emitting phenomena worldwide, such as strombolian and effusive eruptions (Laiolo et al., 2019), open-vent and lava lakes (Massimetti et al., 2020) and explosive lava dome behavior (Shevchenko et al., 2021). The algorithm used here is currently part of two online, automated, near-real time and global volcanic monitoring systems: the MIROVA thermal monitoring system (based on MODIS MIR data, Coppola et al., 2016a, b), and the multiparametric MOUNTS project (presented above; Valade et al., 2019), and was the first SWIR Sentinel-2 thermal algorithm operationally online and publicly available (Massimetti et al., 2020).

Results and Discussion

Pléiades

Lava flow field characterization

Figure 3 is an example of a multispectral image (left panel) derived from the Pléiades stereo-images acquired on the 30th of March. It shows the lava flow footprint with hot spots in red color located at the center of the lava flow unit, and cooled areas in black around it. On the right panel, we provide the lava thickness map with volume of magma emitted and surface footprint. 11 days after the eruption start, the active center part of the lava flow reaches a maximum thickness of 35 m, for a surface of 0.29 km^2, leading to a lava volume of 4.8 Mm^3 at this

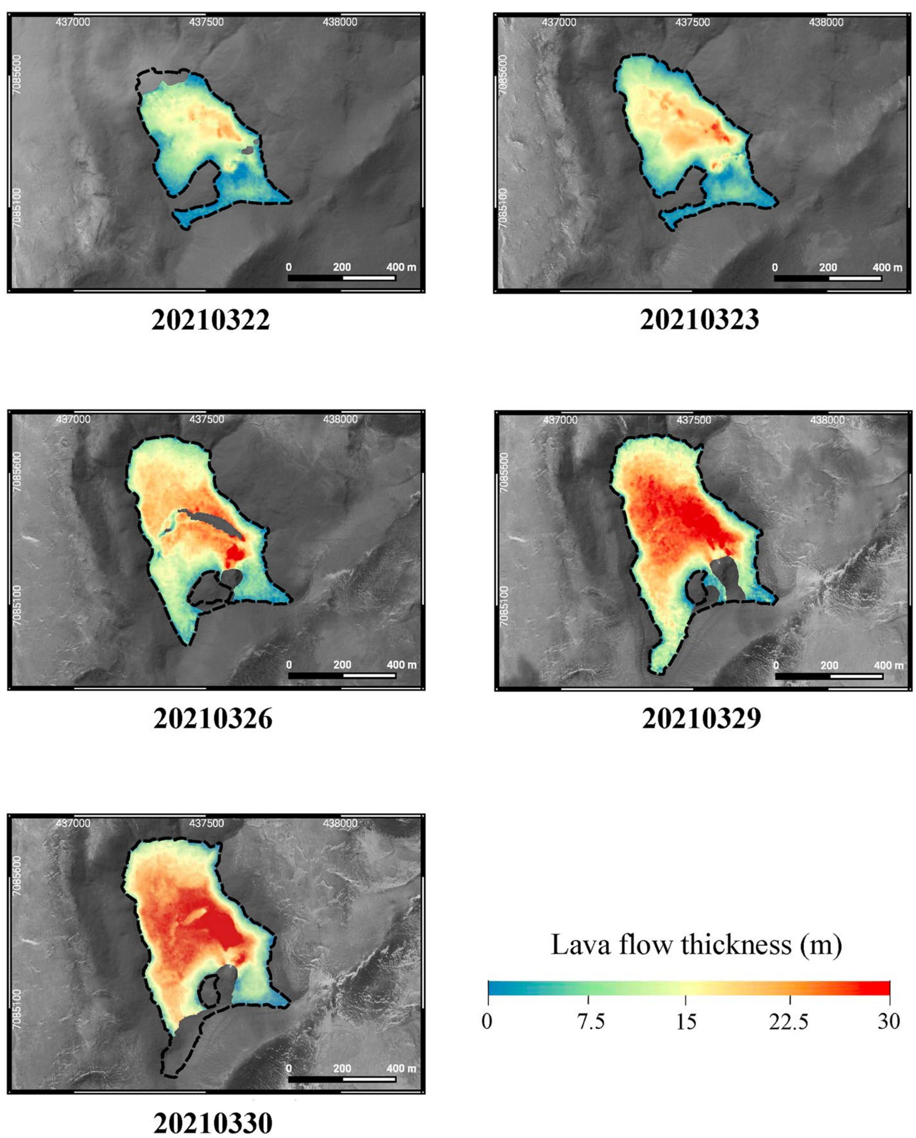

Fig. 5 Lava thickness maps obtained after reanalysis for the 5 Pléiades acquisitions listed in Table 2. Background Pléiades orthorectified images. © CNES 2021, Distribution Airbus DS

time point of magma emitted. This information was provided to the Icelandic Civil Protection about 6 h after the image acquisition.

All successive volumes and effusion rates (22, 23, 26, 29, 30, and 31 March) estimated in the response mode either from Pléiades images or airborne surveys are listed in Table 2 together with those estimated by reanalysis and represented in Fig. 4. Reanalysis data are very close to the ones of the response mode showing the robustness of operational routines used which is essential for rapid and reliable response of the Civil Protection Authorities. The data presented demonstrate that the cumulative volume (Fig. 4) increases almost linearly with time having a lava effusion rate ranging from 5–6 m^3/s. In more details, the accuracy of Pléiades data allows us to witness a small but significant decrease of the lava effusion rate from 6.2 m^3/s on the 22nd of March to 5.3 m^3/s on the 30th of March (Fig. 4). Interestingly, the two lava volumes provided by airborne data are in very good agreement with the Pléiades results. Indeed, lava volumes derived from airborne data on 22/03 (1010UTC) is 1.72 Mm^3 while the Pléiades one, ~3 hours later (1315UTC) on the same day, is 1.84 Mm^3. Airborne results, seen here as ground truth, demonstrate the accuracy of Pléiades data, and reinforce the objective of the CIEST^2 initiative as using Pléiades images for operational purposes. Figure 5 presents all the thickness maps derived from Pléiades data in the reanalysis mode. From Table 2 and Fig. 4, it appears here again that there is no significant difference between volumes estimated in response mode and those estimated afterwards during the reanalysis (differences are within error bars). We can thus conclude that the response mode was efficient at providing a quick and rather accurate estimation to the Icelandic Civil Protection. For the airborne survey, the reanalysis slightly modified the estimation of volume derived from the survey performed on the 23rd of March whereas it didn't change significantly the estimation derived from the one made on the 31st of March. The thickness distribution agreement derived from Pléiades images and the airborne survey has been tested as a thickness difference map (Fig. 6) on 23 March, where the Pléiades acquisition was performed 3 h only after the airborne survey. The result is important, as no significant elevation difference remains overall, except at the location of

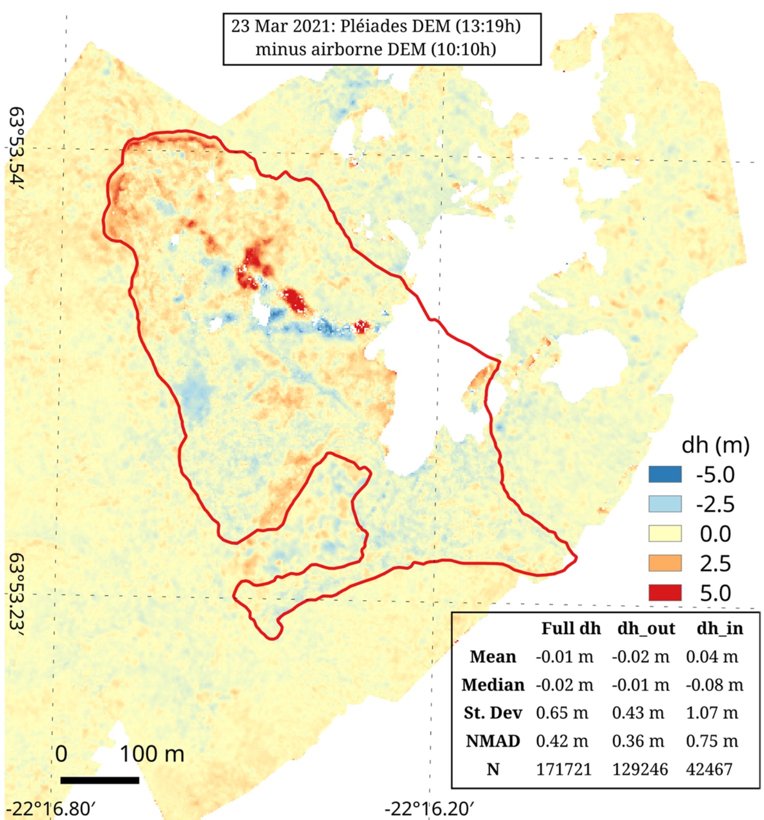

Fig. 6 Difference in elevation between the two surveys from 23 March (Pléiades and airborne DEMs), in reanalysis mode. Red colors indicate thickening, as in the NW lobes of the eruption

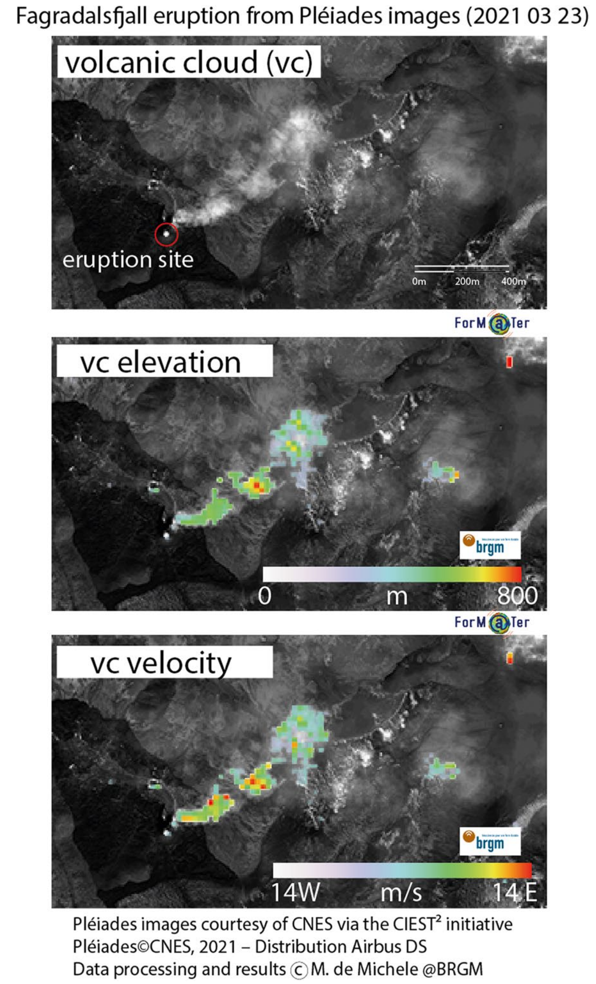

Fig. 7 Plume Elevation Model of Fagradalsfjall, results from the 23rd of March 2021: top) Pléiades image, panchromatic band; middle) produced elevation map; bottom) produced velocity map. Pléiades images courtesy of CNES via CIEST², © CNES 2021, Distribution Airbus DS

the active vents of lava emission, where effusion rates are high enough to build a detectable change in lava flow elevation in about 3 h.

Volcanic plume characterization

Volcanic plume altitude estimation is essential as it provides information on eruption source parameters and dynamics, and is essential for air traffic risks mitigation. In this regard, the Plume Elevation Model (PEM) as calculated from Pléiades is very accurate and can be reliably used. In Fig. 7, we presents the results of the PEM from a volcanic cloud imaged on the 23rd of March 2021 by Pléiades. The altitude of the volcanic cloud varies between 300 and 800 m above sea level. This is a weak buoyant plume, mostly composed of condensed water, and probably sulfuric acid droplets with little or no ash (Barnie et al., 2022). The trajectory of such a volcanic plume is fully controlled by the wind. The maximum velocity of the volcanic plume displacement reaches 14 m/s, which is in accordance with observations made with the Global Forecast System (GFS) by National Oceanic and Atmospheric administration (NOAA), visualized with Ventusky web platform (https://www.ventusky.com/).

Meteosat-SEVIRI

As a geostationary platform, the MSG-SEVIRI satellite allows rapid detection of lava hot spots as well as the estimation of quantitative parameters such as lava volume and lava effusion rates. This operational effort is currently being carried out by the HOTVOLC web-service, especially for Icelandic targets where volcanic eruptions are frequent. Therefore, results presented here directly come from data of the HOTVOLC platform, i.e., in crisis response mode, and no offline processing has been carried out for this particular case. This fills the main objective of the paper, that is, to show how satellite data can assist rapid decision making and response with online data using operational routines.

In Fig. 8, we show a time series of the lava Volume Flow Rate (VFR in m^3/s) for the first 10 days of the eruption, associated with the cumulative lava volume over the same period. The first detection occurred at 21h15 UTC on 19 March with a VFR of 5.3 m^3/s, that is, less than one hour after the eruption start. The related hot spot detection is visible in real-time on the HOTVOLC interface, and associated with a color code scaled to the spectral radiance amplitude. Detections were scarce during the following two days likely due to the presence of a volcanic plume above the source vents. Then, the rate of acquisition improves to one image every 15 min and shows an increase of the VFR up to 20–30 m^3/s around 23 March. Then, the VFR decreases to values in the range 5–10 m^3/s for the rest of the period with some peaks at around 15 m^3/s. The time evolution of the VFR can also be read through the cumulative lava volume slope, first increasing, and then decreasing. On March 30, the total volume emitted and estimated using MSG-SEVIRI is ~ 5.23 Mm^3, and corresponding to an average effusion rate over the ten days of 5.93 m^3/s. In Fig. 8, we also compare cumulative lava volume from MSG-SEVIRI, Pléiades and airborne data. Related volumes estimations are quite close and show a similar time evolution, with all values derived from MSG-SEVIRI being slightly larger than the ones derived from other methods. All results are summarized in Table 3 in the conclusion section.

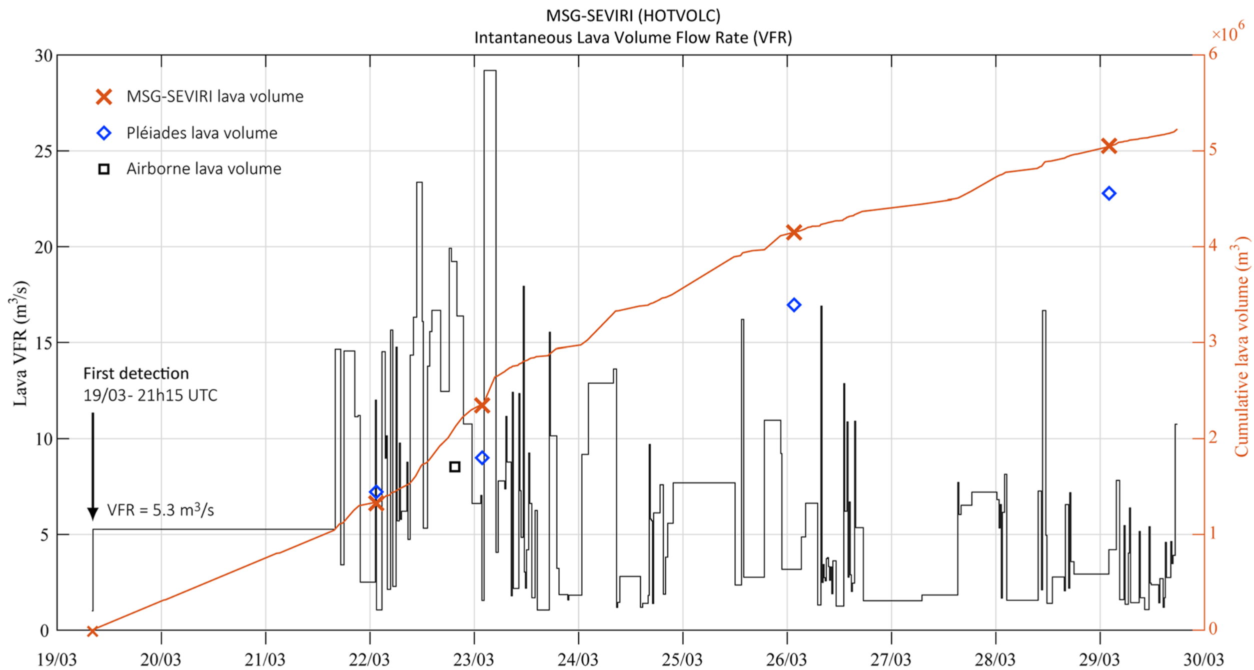

Fig. 8 time series of the instantaneous lava Volume Flow Rate (VFR in m^3/s) and cumulative lava volume (m^3) during the first 10 days of the eruption, with landmarks showing acquisition times of Pléiades images

Sentinel-2

Here we present Sentinel-2 MSI images (S2 hereafter) processed by MOUNTS, with the aim to show the contribution of these products having an intermediate spatial and temporal resolution with respect to Pléiades and Meteosat products. As the effusive eruption began on 19 March from a ~ 150 m long fissure inside the Geldingadalir valley, and evolved to a larger crater with two main vents, the spatial resolution of S2 products is appropriate to map and observe the evolution of the lava field. We show the first two cloud-free images, depicting the first stage of the eruption, acquired on the 23rd of March 2021 (13:02 UTC) and the 30th of March 2021 (13:12 UTC). Other S2 images were acquired on March 25 and 28. However the thick and pervasive cloud coverage does not allow proper visualization of the evolving lava field. The images are presented in Fig. 9, with three different visualizations: i) 10x10 km image with a combination of optical bands and SWIR bands, highlighting the presence of hot materials over background and to appreciate the surrounding environmental features; ii) a 2x2 km zoom with a combination of optical and SWIR bands, only for the pixel detected by the algorithm as hot; iii) a 2x2 km side zoom solely with the SWIR contribution.

The hot spot algorithm automatically detected on 23 March a total of 920 hot pixels, and on 30 March a total of 686 pixels. These can be converted into “hot” area by multiplying by the pixel area (20X20 m^2) of the

Table 3 Summary of the quantitative information on the lava flow evolution provided by the various independent remote sensing datasets considered in this study

Date	Pléiades			Airborne			Meteosat		Sentinel-2
	Area km^2	Vol Mm^3	Avg Eff. rate m^3/s	Areakm^2	Vol Mm^3	Avg Eff. Rate m^3/s	Vol Mm^3	Avg Eff. Rate m^3/s	Area km^2
20,210,322	0.17	1.43	6.2	-	-	-	1.34	5.75	-
20,210,323	0.17	1.84	5.8	0.19	1.72	5.6	2.35	7.34	0.37
20,210,326	0.19	3.30	5.7	-	-	-	4.14	7.28	-
20,210,329	0.24	4.57	5.4	-	-	-	5.04	6.12	-
20,210,330	0.28	4.89	5.3	-	-	-	5.23	5.93	0.27
20,210,331	-	-	-	0.30	5.23	5.2	-	-	-

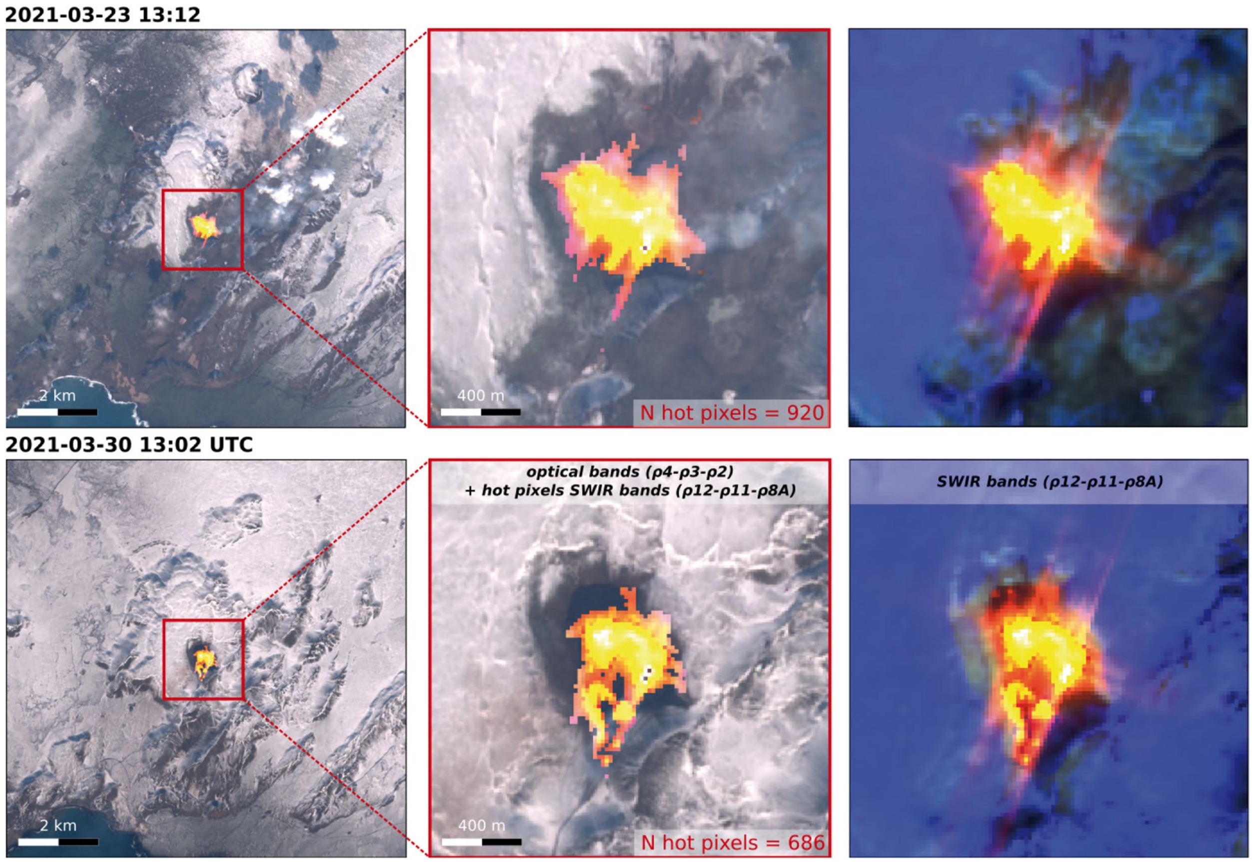

Fig. 9 Cloud-free Sentinel-2 images acquired during the first 10 days of the eruption. Left panel is a 10x10 km image with a combination of optical bands and SWIR bands (i.e., "hot" pixel detected by the algorithm are displayed using the SWIR bands), middle panel is a 2x2 km zoom, right panel is a 2x2 km zoom with solely SWIR band combination

Sentinel 2 SWIR bands. The converted area thus resulted in 0.368 km^2 and 0.274 km^2 for 23 March and 30 March, respectively.

The two S2 images, acquired 7 days apart, allow monitoring of the lava flow field evolution. The first image shows a single and unique thermal anomaly expanding around the main eruptive fissure, while the second presents an already partially evolved lava area, with some portions already cooled and crusted (NNW), a portion still hot and active around the main vents, and the first stage of lava flow moving towards the South.

As described in Massimetti et al. (2020) and visible in Fig. 9, the number of hot pixels detected over highly radiative bodies such as lava flows can sometimes be overestimated, in particular due to halo effects and artifacts on the MSI detector (i.e., diffraction spikes triggered by instrument optics effects and intense thermal emissions, particularly visible on the March 23 acquisition). Nevertheless, the lava flow area estimated by S2 seems in good agreement with Pléiades image acquired on the 30th of March 2021 (see Fig. 3), with a final estimate of 0.29 km^2.

Conclusion

The first part of the ongoing effusive eruption at Fagradalsfjall on Reykjanes Peninsula, (Iceland) that began March 19, 2021, was closely monitored in near-real time by photogrammetry using high-resolution optical Pléiades stereo images. Key information such as the lava flow outlines, thickness maps, volumes and average effusion rates were provided to the civil protection in less than 6 h after the data acquisition, which was useful for hazard evaluation, aided in the development of scenarios on potential impact on infrastructure, and helped to manage tourism resulting from this spectacular eruption not far from of the Icelandic capital city.

To our knowledge, this is the first time that stereo High Resolution optical satellite data are used in an operational way for eruption monitoring. The absence of prior usage for hazard monitoring is probably linked to non-systematic availability of these datasets. For the Fagradalsfjall eruption, Pléiades acquisitions were available, during the first ten days of the event, thanks to a special tasking request made to Airbus DS by CNES after the CIEST^2 activation. We benefited from a favorable situation where the eruptive event had been anticipated and weather conditions during this period were quite good. The systematic acquisitions over the eruption site lasted for 10 days but additional stereo Pléiades images have been acquired subsequently (28th of April and 2nd of July) by the Icelandic Volcanoes Supersite project supported by the Committee on Earth Observing Satellites or by commercial requests.

Both the subsequent reanalysis of the results produced initially in an operational way and the comparison with area, thickness, volume, and effusion rates derived from airborne surveys validate the near-real time estimations obtained in “response mode” and rapidly provided to local authorities for crisis management. In addition, Pléiades images have the potential to provide useful complementary information on the state of the volcanic plume (elevation and velocity). For the response mode, we relied on local processing chains, quickly adjusting off-the-shelf tools. Indeed, operational monitoring platforms for volcanic activity like MOUNTS or HOTVOLC usually takes advantage of systematic and freely distributed satellite acquisitions. In this study, by comparing the lava flow area and effusion rate estimations derived from Pléiades images with, respectively, the area and effusion rates obtained from respectively Sentinel-2 data and from MSG-SEVIRI data, we confirmed the potential of these open-access platforms to quantitatively provide robust real-time information for effusive eruption monitoring (see Table 3 for a summary of results obtained by various independent methods).

The eruption of Fagradalsfjall 2021 is a proof of concept of the added value of satellite data for volcano monitoring. It shows that despite the strong potential of routinely acquired satellite data (Copernicus, MSG) and their efficient exploitation via online and open access platforms, access and availability of high resolution data such as Pléiades imagery can be of major importance in developing operational processing chains dedicated to these particular data. In this perspective, the DSM-OPT online service of ForM@ter operated by EOST has been improved to automatically produce DEMs from Pléiades stereo images as soon as they are delivered by Airbus DS after activation by CIEST^2. Since the Icelandic eruption, CIEST^2 has also enabled Pléiades acquisition for the St Vincent Soufrière eruption in April 2021 and for the Nyiragongo eruption in May 2021.

Acknowledgements
HOTVOLC data processing performed by MG and YG was supported by French CNRS-INSU through the National Observation Service in Volcanolgy (SNOV), and the French Space Agency named Centre National d’Études Spatiales (CNES). Pléiades images have been acquired thanks to the CNES via CIEST^2 (© CNES 2021, Distribution Airbus DS), CIEST^2 is part of ForM@Ter (https://en.poleterresolide.fr/) and supported by ISDeform National Observation Service. VP was supported by the CNES project MagmaTrack. We also thank the handling editor for helpful corrections.

Authors’ contributions
MG designed the paper and planned the research. VP, SG, JB and EB processed Pléiades data for lava volume and effusion rates. MdM and DR processed Pléiades data for volcanic plume study. CP and CT helped with fast Pléiades acquisition through the CIEST^2 consortium. MG and YG processed IR data from HOTVOLC platform (MSG-SEVIRI). MTG, BO and BO led the operational survey for airborne data acquisition and processing. SV and FM processed sentinel-2 data.

Funding
Sentinel-2 data processing associated with SV’s work was funded thanks to the PAPIIT project IA102221.

Availability of data and materials
The datasets used and/or analyzed during the current study are available from the corresponding author on.
reasonable request.

Declarations

Competing interest
The authors declare that they have no competing interests.

Author details
[1]Université Clermont Auvergne, CNRS, F-63000 Clermont-Ferrand, IRD, OPGC, LMV, France. [2]Virginie Pinel- University Grenoble Alpes, University Savoie Mont Blanc, CNRS, UGE, ISTerre, Grenoble, IRD, France. [3]National Land Survey of Iceland, Akranes, Iceland. [4]Institute of Earth Sciences, University of Iceland, Reykjavík, Iceland. [5]BRGM, Risks and Prevention Department, Geophysical Imagery and Remote Sensing Unit, 3 avenue Claude Guillemin, 45060 Orléans, France. [6]CNES: Centre National d’Études Spatiales, Toulouse, France. [7]LEGOS Université de Toulouse, CNES, CNRS, UPS, Toulouse, IRD, France. [8]Icelandic Institute of Natural History,, Garðabær, Iceland. [9]University Grenoble Alpes, University Savoie Mont Blanc, CNRS, UGE, ISTerre, Grenoble, IRD, France. [10]Departamento de Vulcanología, Instituto de Geofísica, Universidad Nacional Autónoma de México UNAM, Mexico City, Mexico. [11]Department of Earth Sciences, University of Torino, Via Valperga Caluso 35, 10125 Turino, Italy. [12]Department of Civil Protection and Emergency Management, National Commissioner of the Icelandic Police, Reykjavík, Iceland.

Received: 17 September 2021 Accepted: 11 July 2022
Published online: 13 August 2022

References
Porter, C., Morin, P., Howat, I., et al. ArcticDEM. Harvard Dataverse, 2018, vol. 1, p. 2018-30.08.
Shean, D: E., Bhushan, S. (2021). Chamoli Disaster Pre-event DEM (2015-05-07 WorldView-1 Stereo). https://zenodo.org/record/4533679#.YNM73DrLeV4
Shean, D: E., Bhushan, S., Berthier, E., Deschamps-Berger, C., Gascoin, S., Knuth, F. (2021). Chamoli Disaster Post-event 2-m DEM Composite (February 10-11, 2021) and Difference Map. https://zenodo.org/record/4558692
Aiuppa A, Fiorani L, Santoro S, Parracino S, Nuvoli M, Chiodini G, Tamburello G (2015) New ground-based lidar enables volcanic CO 2 flux measurements. Sci Rep 5(1):1–12
Albino F, Smets B, d’Oreye N, Kervyn F (2015) High-resolution TanDEM-X DEM: An accurate method to estimate lava flow volumes at Nyamulagira Volcano (DR Congo). Journal of Geophysical Research: Solid Earth 120(6):4189–4207

F. Albino, J. Biggs, R. Escobar-Wolf, A. Naismith, M. Watson, J.C. Phillips, G.A. Chigna Marroquin, Using TanDEM-X to measure pyroclastic flow source location, thickness and volume: Application to the 3rd June 2018 eruption of Fuego volcano, Guatemala, Journal of Volcanology and Geothermal Research, Volume 406, 2020
Albino, F., Biggs, J., Yu, C., & Li, Z. (2020). Automated Methods for Detecting Volcanic Deformation Using Sentinel-1 InSAR Time Series Illustrated by the 2017–2018 Unrest at Agung, Indonesia. Journal of Geophysical Research: Solid Earth, 125(2), e2019JB017908.
Allen AG, Baxter PJ, Ottley CJ (2000) Gas and particle emissions from Soufrière Hills Volcano, Montserrat, West Indies: characterization and health hazard assessment. Bull Volcanol 62(1):8–19
Arnold D, Biggs J, Anderson K, Vallejo Vargas S, Wadge G, Ebmeier S, Naranjo M, Mothes P (2017) Decaying lava extrusion rate at El Reventador Volcano, Ecuador, measured using high-resolution satellite radar. J Geophys Res Solid Earth 122:9966–9988
Bagnardi M, Gonzalez PJ, Hooper A (2016) High-resolution digital elevation model from tri-stereo Pléiades-1 satellite imagery for lava flow volume estimates at Fogo volcano. Geophys Res Lett 43(12):6267–6275
Barnie, T., Titos, M., Hjörvar, T., Bergsson, B., Pálsson, S., Oddson, B., ... & Arason, Þ. (2022). Monitoring volcanic plume height and fountain height using webcameras at the 2021 Fagradalsfjall eruption in Iceland (No. EGU22–12260). Copernicus Meetings.
Barsotti S, Oddsson B, Gudmundsson MT, Pfeffer MA, Parks MM, Ófeigsson BG, Vogfjörd K (2020) Operational response and hazards assessment during the 2014–2015 volcanic crisis at Bárðarbunga volcano and associated eruption at Holuhraun, Iceland. J Volcanol Geoth Res 390:106753
Bato MG, Froger JL, Harris AJL, Villeneuve N (2016) Monitoring an effusive eruption at Piton de la Fournaise using radar and thermal infrared remote sensing data: insights into the October 2010 eruption and its lava flows. In: Harris AJL, De Groeve T, Garel F, Carn SA (eds) Detecting. Geological Society, London, Special Publications, Modelling and Responding to Effusive Eruptions, p 426
Belart J, Magnusson J, Berthier E, Palsson F, Adalgeirsdottir G, Johannesson (2019) The geodetic mass balance of Eyjafjallajökull ice cap for 1945–2014: Processing guidelines and relation to climate. J Glaciol 65(251):395–409. https://doi.org/10.1017/jog.2019.16
Berthier E, Arnaud Y, Kumar R, Ahmad S, Wagnon P, Chevallier P (2007) Remote sensing estimates of glacier mass balances in the Himachal Pradesh (Western Himalaya, India). Remote Sens Environ 108:327–338. https://doi.org/10.1016/j.rse.2006.11.017
Blackett M (2017) An Overview of Infrared Remote Sensing of Volcanic Activity. Journal of Imaging 3(2):13. https://doi.org/10.3390/jimaging3020013
Bonadonna, C., Genco, R., Gouhier, M., Pistolesi, M., Cioni, R., Alfano, F., ... & Ripepe, M. (2011). Tephra sedimentation during the 2010 Eyjafjallajökull eruption (Iceland) from deposit, radar, and satellite observations. Journal of Geophysical Research: Solid Earth, 116(B12).
Calvari, S., Salerno, G. G., Spampinato, L., Gouhier, M., La Spina, A., Pecora, E., ... & Boschi, E. (2011). An unloading foam model to constrain Etna's 11–13 January 2011 lava fountaining episode. Journal of Geophysical Research: Solid Earth, 116(B11).
Carrara A, Pinel V, Bascou P, Chaljub E, la Cruz-Reyna SD (2019) Post-emplacement dynamics of andesitic lava flows at volcan de Colima, Mexico, revealed by radar and optical remote sensing data. J Volcanol Geoth Res 381:1–15
Coppola D, Laiolo M, Cigolini C (2016a) Fifteen years of thermal activity at Vanuatu's volcanoes (2000–2015) revealed by MIROVA. J Volcanol Geotherm Res 322:6–19
Coppola D, Laiolo M, Cigolini C, Delle Donne D, Ripepe M (2016b) Enhanced volcanic hot-spot detection using MODIS IR data: results from the MIROVA system. Geological Society, London, Special Publications 426(1):181–205
de Michele M, Raucoules D, Arason Þ (2016) Volcanic plume elevation model and its velocity derived from Landsat 8. Remote Sens Environ 176:219–224
Deschamps-Berger C, Gascoin S, Berthier E, Deems J, Gutmann E, Dehecq A, Shean D, Dumont M (2020) Snow depth mapping from stereo satellite imagery in mountainous terrain: evaluation using airborne laser-scanning data. Cryosphere 14(9):2925–2940. https://doi.org/10.5194/tc-14-2925-2020
Di Traglia F, De Luca C, Manzo M, Nolesini T, Casagli N, Lanari R, Casu F (2021) Joint exploitation of space-borne and ground-based multitemporal InSAR measurements for volcano monitoring: The Stromboli volcano case study. Remote Sens Environ 260:112441
Dumont S, Sigmundsson F, Parks MM, Drouin VJ, Pedersen G, Jónsdóttir I, Oddsson B (2018) Integration of SAR data into monitoring of the 2014–2015 Holuhraun eruption, Iceland: contribution of the Icelandic volcanoes supersite and the FutureVolc projects. Front Earth Sci 6:231
Ebmeier SK, Biggs J, Mather TA, Elliott JR, Wadge G, Amelung F (2012) Measuring large topographic change with InSAR: Lava thicknesses, extrusion rate and subsidence rate at Santiaguito volcano, Guatemala. Earth Planet Sci Lett 335:216–225
Flynn LP, Wright R, Garbeil H, Harris A, Pilger E (2002) A global thermal alert system using MODIS: initial results from 2000–2001. Advances in Environmental Monitoring and Modelling 1(1):37–60
Ganci G, Vicari A, Cappello A, Del Negro C (2012) An emergent strategy for volcano hazard assessment: from thermal satellite monitoring to lava flow modeling. Remote Sens Environ 119:197–207
Ganci, G., Cappello, A., Bilotta, G., Corradino, C., Del Negro, C., 2019a. Satellite-based reconstruction of the volcanic deposits during the December 2015 Etna eruption. Data4, 120. 10 .3390 /data4030120.
Girod L, Nuth C, Kääb A, McNabb R, Galland O (2017) MMASTER: Improved ASTER DEMs for Elevation Change Monitoring. Remote Sensing 9(7):704. https://doi.org/10.3390/rs9070704
Gouhier M, Harris A, Calvari S, Labazuy P, Guéhenneux Y, Donnadieu F, Valade S (2012) Lava discharge during Etna's January 2011 fire fountain tracked using MSG-SEVIRI. Bull Volcanol 74(4):787–793
Gouhier M, Guéhenneux Y, Labazuy P, Cacault P, Decriem J, Rivet S (2016) HOTVOLC: A web-based monitoring system for volcanic hot spots. Geological Society, London, Special Publications 426(1):223–241
Gouhier M, Deslandes M, Guéhenneux Y, Hereil P, Cacault P, Josse B (2020) Operational Response to Volcanic Ash Risks Using HOTVOLC Satellite-Based System and MOCAGE-Accident Model at the Toulouse VAAC. Atmosphere 11(8):864
Harris A (2013) Thermal Remote Sensing of Active Volcanoes. Cambridge University Press, Cambridge, UK
Höhle J, Höhle M (2009) Accuracy assessment of digital elevation models by means of robust statistical methods. ISPRS J Photogramm Remote Sens 64:398–406. https://doi.org/10.1016/j.isprsjprs.2009.02.003
Kelfoun K, Santoso AB, Latchimy T, Bontemps M, Nurdien I, Beauducel F, Gueugneau V (2021) Growth and collapse of the 2018–2019 lava dome of Merapi volcano. Bull Volcanol 83(2):1–13
Kubanek J (2017) Westerhaus, Malte, Heck, Bernhard, TanDEM-X Time Series Analysis Reveals Lava Flow Volume and Effusion Rates of the 2012–2013 Tolbachik. Kamchatka Fissure Eruption, Journal of Geophysical Research: Solid Earth 122(10):7754–7774
Kubanek J, Westerhaus M, Schenk A, Aisyah N, Brotopuspito KS, Heck B (2015) Volumetric change quantification of the 2010 Merapi eruption using TanDEM-X InSAR. Remote Sens Environ 164:16–25
Labazuy P, Gouhier M, Harris A, Guéhenneux Y, Hervo M, Bergès JC, Rivet S (2012) Near real-time monitoring of the April–May 2010 Eyjafjallajökull ash cloud: an example of a web-based, satellite data-driven, reporting system. Int J Environ Pollut 48(1–4):262–272
Laiolo, M.; Ripepe, M.; Cigolini, C.; Coppola, D.; Della Schiava, M.; Genco, R.; Innocenti, L.; Lacanna, G.; Marchetti, E.; Massimetti, F.; et al. Space-and Ground-Based Geophysical Data Tracking of Magma Migration in Shallow Feeding System of Mount Etna Volcano. Remote Sens. 2019, 11, 1182
Marzano FS, Barbieri S, Vulpiani G, Rose WI (2006) Volcanic ash cloud retrieval by ground-based microwave weather radar. IEEE Trans Geosci Remote Sens 44(11):3235–3246
Massimetti F, Coppola D, Laiolo M, Valade S, Cigolini C, Ripepe M (2020) Volcanic Hot-Spot Detection Using SENTINEL-2: A Comparison with MODIS–MIROVA Thermal Data Series. Remote Sensing 12(5):820. https://doi.org/10.3390/rs12050820
de Michele, M.; Raucoules, D.; Corradini, S.; Merucci, L.; Salerno, G.; Sellitto, P.; Carboni, E. Volcanic Cloud Top Height Estimation Using the Plume Elevation Model Procedure Applied to Orthorectified Landsat 8 Data. Test Case: 26 October 2013 Mt. Etna Eruption. Remote Sens. 2019, 11, 785. https://doi.org/10.3390/rs11070785
Moussallam, Y. Barnie, B., Amigo, A., Kelfoun, K., Flores, F., Franco, L., Cardona, C., Cordova, L., Toloza, T., Monitoring and forecasting hazards from a slow

growing lava dome using aerial imagery, tri-stereo Pléiades-1A/B imagery and PDC numerical simulation, Earth and Planetary Science Letters, Volume 564, 2021.
Nuth C, Kääb A (2011) Co-registration and bias corrections of satellite elevation data sets for quantifying glacier thickness change. Cryosphere 5:271–290. https://doi.org/10.5194/tc-5-271-2011
Pedersen GBM, Belart JMC, Óskarsson BV, Gudmundsson MT, Gies N, Högnadóttir Th, Hjartardóttir AR, Pinel V, Berthier E, Dürig T, Reynolds HI, Hamilton CW, Valsson G, Einarsson P, Ben-Yehosua D, Gunnarsson D, Oddsson, B.: Volume, effusion rate, and lava transport during the (2021) Fagradalsfjall eruption: Results from near real-time photogrammetric monitoring. Geophisical Research Letters (in Press). https://doi.org/10.1029/2021GL097125
Peltier A, Ferrazzini V, Di Muro A, Kowalski P, Villeneuve N, Richter N, Ramsey M (2021) Volcano crisis management at Piton de la Fournaise (La Réunion) during the COVID-19 lockdown. Seismological Society of America 92(1):38–52
Pierrot-Deseilligny M (2011) Clery I. Apero, an Open Source Bundle Adjustment Software for Automatic Calibration and Orientation of Set of Images 38(5):269–276
Pinel, V., Putra, R., Solikhin, A., Beauducel, F., Santoso, A. B., Humaida, H. Tracking the evolution of the Merapi volcano crater area by high-resolution satellite, Geophysical Research Abstracts, Vol. 22, EGU2020–5415, 2020, EGU General Assembly 2020.
Poland MP (2014) Time-averaged discharge rate of subaerial lava at Klauea Volcano, Hawai'i, measured from TanDEM-X interferometry: Implications for magma supply and storage during 2011–2013. J Geophys Res Solid Earth 119:5464–5481
Richter N, Froger JL (2020) The role of Interferometric Synthetic Aperture Radar in detecting, mapping, monitoring, and modelling the volcanic activity of Piton de la Fournaise. La Réunion: A Review Remote Sensing 12(6):1019
Rupnik, E., Daakir, M. and Pierrot-Deseilligny, M. P. (2017). Micmac–a free, open-source solution for pho- togrammetry. Open Geospatial Data, Software and Standards, 2(1):1–9. https://opengeospatialdata.springeropen.com/articles/https://doi.org/10.1186/s40965-017-0027-2
Schmidt A, Leadbetter S, Theys N, Carboni E, Witham CS, Stevenson JA, Shepherd J (2015) Satellite detection, long-range transport, and air quality impacts of volcanic sulfur dioxide from the 2014–2015 flood lava eruption at Bárðarbunga (Iceland). Journal of Geophysical Research: Atmospheres 120(18):9739–9757
Scollo, S., Prestifilippo, M., Bonadonna, C., Cioni, R., Corradini, S., Degruyter, W., ... & Pecora, E. (2019). Near-Real-Time Tephra Fallout Assessment at Mt. Etna, Italy. Remote Sensing, 11(24), 2987.
Shean DE, Alexandrov O, Moratto ZM, Smith BE, Joughin IR, Porter C, Morin P (2016) An automated, open-source pipeline for mass production of digital elevation models (DEMs) from very-high-resolution commercial stereo satellite imagery. ISPRS J Photogramm Remote Sens 116:101–117. https://doi.org/10.1016/j.isprsjprs.2016.03.012
Shean DE, Bhushan S, Montesano P, Rounce DR, Arendt A, Osmanoglu B (2020) A Systematic, Regional Assessment of High Mountain Asia Glacier Mass Balance. Front Earth Sci 7:363. https://doi.org/10.3389/feart.2019.00363
Shevchenko, Alina V., Dvigalo, Viktor N., Zorn, Edgar U., Vassileva, Magdalena S., Massimetti, Francesco, Walter, Thomas R., Svirid, Ilya Yu., Chirkov, Sergey A., Ozerov, Alexey Yu., Tsvetkov, Valery A., Borisov, Ilya A, (2021) Constructive and Destructive Processes During the 2018–2019 Eruption Episode at Shiveluch Volcano, Kamchatka, Studied From Satellite and Aerial Data, Frontiers in Earth Science, https://www.frontiersin.org/article/10.3389/feart.2021.680051
Thivet, S., Gurioli, L., Di Muro, A., Derrien, A., Ferrazzini, V., Gouhier, M., ... & Arellano, S. (2020). Evidences of plug pressurization enhancing magma fragmentation during the September 2016 basaltic eruption at Piton de la Fournaise (La Réunion Island, France). Geochemistry, Geophysics, Geosystems, 21(2), e2019GC008611.
Valade S, Ley A, Massimetti F, D'Hondt O, Laiolo M, Coppola D, Loibl D, Hellwich O, Walter TR (2019) Towards Global Volcano Monitoring Using Multisensor Sentinel Missions and Artificial Intelligence: The MOUNTS Monitoring System. Remote Sensing 11(13):1528. https://doi.org/10.3390/rs11131528
Vicari, A., Bilotta, G., Bonfiglio, S., Cappello, A., Ganci, G., Hérault, A., ... & Del Negro, C. (2011). LAV@ HAZARD: a web-GIS interface for volcanic hazard assessment. Annals of Geophysics, 54(5).
Wright R, Blake S, Harris AJ, Rothery DA (2001) A simple explanation for the space-based calculation of lava eruption rates. Earth Planet Sci Lett 192(2):223–233
Wright R, Flynn L, Garbeil H, Harris A, Pilger E (2002) Automated volcanic eruption detection using MODIS. Remote Sens Environ 82(1):135–155

Publisher's Note

Springer Nature remains neutral with regard to jurisdictional claims in published maps and institutional affiliations.